NANOSYSTEMS:
PHYSICS, CHEMISTRY, MATHEMATICS

Boleiko G.M., et al. *Nanosystems: Phys. Chem. Math.*, 2025, **16** (1), 44–50.
http://nanojournal.ifmo.ru
**DOI 10.17586/2220-8054-2025-16-1-44-50**

Original article

# Synthesis and characterization of $InGaZn_2O_5$ obtained by nitrate-tartrate complex decomposition method

Gelena M. Boleiko[1,a], Gleb M. Zirnik[1,b], Andrey I. Kovalev[1,2,c], Daniil A. Uchaev[2,d], Ibrohimi A. Solizoda[1,3,4,e], Alexander S. Chernukha[1,2,f], Svetlana A. Gudkova[1,3,g], Denis A. Vinnik[1,2,3,h]

[1]Moscow Institute of Physics and Technology Institutsky lane, 9, Dolgoprudny, 141701, Russia

[2]South Ural State University, Lenin Av., 76, Chelyabinsk, 454080, Russia

[3]St. Petersburg State University Universitetskaya embankment, 7-9, 199034, St. Petersburg

[4]Tajik National University Rudaki Av., 17, Dushanbe, 734025, Tajikistan

[a]boleiko.gm@mipt.ru, [b]glebanaz@mail.ru, [c]asp23kai165@susu.ru, [d]uchaevda@susu.ac.ru, [e]solizoda.ia@mipt.ru, [f]chernukha.as@mipt.ru, [g]svetlanagudkova@yandex.ru, [h]vinnik.da@mipt.ru

Corresponding author: D. A. Vinnik, vinnik.da@mipt.ru

ABSTRACT The study for the first time presents a method for producing indium-gallium-zinc oxide $InGaZn_2O_5$ using the nitrate-tartrate complex decomposition method. The material is characterized by X-ray diffraction, electron microscopy, IR- and UV-spectroscopy. It has been established that the use of tartaric acid as a precursor already at a temperature of 500 °C leads to the formation of a single-phase homogeneous material consisting of nanocrystalline particles in the form of micrometer agglomerates. The proposed method for producing nanoparticles can be used in the future to produce semiconductor inks based on IGZO.

KEYWORDS indium-gallium-zinc oxide, $InGaZn_2O_5$, IGZO, nanoparticles.

ACKNOWLEDGEMENTS The research is supported by the Ministry of Science and Higher Education of the Russian Federation, project No 075-15-2024-560.

FOR CITATION Boleiko G.M., Zirnik G.M., Kovalev A.I., Uchaev D.A., Solizoda I.A., Chernukha A.S., Gudkova S.A., Vinnik D.A. Synthesis and characterization of $InGaZn_2O_5$ obtained by nitrate-tartrate complex decomposition method. *Nanosystems: Phys. Chem. Math.*, 2025, **16** (1), 44–50.

## 1. Introduction

At present, several main areas of work can be distinguished for obtaining semiconductor materials for further use in semiconductor devices:

1) obtaining one-dimensional Si nanostructures [1];
2) obtaining nano-sized one-dimensional structures of GaAs [2], GaN [3], InAs [4] and others;
3) obtaining metal chalcogenides ($MoS_2$ [5], $WSe_2$ [6], etc.) with two-dimensional morphology;
4) obtaining semiconductor oxide materials (indium tin oxide ITO [7], indium zinc oxide IZO [8], etc.).

Each of these areas covers its own place in terms of material use in the final device. The creation of functional materials for use in electronics, with the aim of developing them towards miniaturisation, is a priority for many research teams around the world. In parallel, the development of printed and flexible electronics is progressing [9–12].

For practical applications, one of the promising oxide materials is amorphous indium gallium zinc oxide [13–15] ($\alpha$–IGZO of various compositions). IGZO (in amorphous state) compares favorably with traditional amorphous silicon due to its higher properties (for example, charge mobility and optical transparency), which ensures both high electrical stability of the material and the flexibility of thin-film transistors based on it. Historically, the possibility of using IGZO as a component to create an electronic device was first demonstrated in the pioneering work of Japanese researchers Nomura and his colleagues [12]. However, in this work, a thin-film transistor was obtained using a single-crystal IGZO layer of the composition $InGaO_3ZnO_5$ on a substrate of single-crystal $ZrO_2$ (stabilized by $Y_2O_3$). Later, the amorphous state of IGZO was also studied. The most promising use of this material was found to be in the form of amorphous thin films [16, 17].

Thin film transistors are used in the new generation of flat panel displays [14, 16–19] and form the basis of devices in all digital systems. Their characteristics, such as carrier mobility ($\mu$), threshold voltage ($V_{th}$), on/off current ratio ($I_{on}/I_{off}$) and subthreshold swing (SS) depend largely on the properties of the semiconductor channel and are determined by the chemical composition, crystallinity, film thickness and the method of obtaining the thin film.

Currently, organic structures are the most popular semiconductors for the production of flexible microelectronic devices. They have become widespread due to the use of high performance technological printing processes and the good quality of the inks produced for printing, the possibility of producing final devices at low temperatures and excellent

compatibility with flexible substrates [20–27]. However, despite these undoubted advantages, the use of organic semiconductors as ink material is limited because final devices on such semiconductors have low technical characteristics, in particular, the mobility of charge carriers in devices using organic semiconductors does not usually exceed 1...2 $cm^2/V{\cdot}s$, which does not allow them to be used for high-power devices. The aspect described above leads to the use of other materials. One of them can be a group of amorphous oxides, for example the ternary oxide IGZO, which has a sufficient set of characteristics of the final device and can be obtained by printing methods. There are several approaches to obtaining materials that would be suitable for ink production. One of these approaches is to obtain "true" non-aggregated nanoparticles in solution and then stabilize them with surfactants to obtain semiconductor ink. For example, there are a number of papers [28, 29] in which the authors have succeeded in obtaining oxide nanoparticles $MeFe_2O_4$ (Me = Mn, Co, Fe) (8...12 nm) of different morphologies (in the form of cubes or hexagons) using Me-acetylacetonate surfactant-mediated decomposition method (the original article did not propose a short name for the method). Theoretically, the use of this synthesis method will potentially allow the stabilized colloidal solutions obtained to be used directly as an ink, without the step of adding surfactants. At the same time, to the best of our knowledge, the described method has not yet been used to obtain indium-gallium-zinc oxide nanoparticles. Despite the excellent results of the Me-acetylacetonate surfactant-mediated decomposition method, which allows obtaining monodisperse nanoparticles, it is poorly scalable, which will lead to difficulties in introducing it into the technological chains of production of these inks in industry.

Another approach is to synthesize nanoparticles using a scalable technology (including solid-phase synthesis [30]), convert the resulting particles to a powder state (in which the nanoparticles are aggregated into large agglomerates) and separate the resulting aggregates using ultrasound treatment or milling methods. This method is not without its drawbacks - during the final stage of milling, it is difficult to obtain a fraction of nanoparticles (their total mass in the final product after milling is about several percents), in addition, the particle size distribution at the final stage of milling becomes random. The above approach can be implemented using the method of decomposition of an organometallic complex (gel) (often called the sol-gel or "solution combustion" method; in the case of using citric acid as a complexing agent, the name "citrate-nitrate" method is common). The essence of the method is to prepare solutions of nitrates of the required metals, form a complex, heat the resulting mixture to remove water and initiate an exothermic self-sustaining oxidation reaction of the complex to yield the target product (called as self-combustion synthesis). The synthesis method is well scalable and relatively simple, allowing the production of agglomerates of IGZO nanoparticles in an amorphous (X-ray amorphous) state under low temperature conditions.

In the literature, works on obtaining thin films (using spin-coating technology with subsequent initiation of the spontaneous combustion reaction) are mostly presented, where 2-methoxyethanol [31] and urea [32] are used as complexing agents. However, it is also possible to use ready-made organometallic complexes - metal acetylacetonates [33]. The authors proposed an approach using a mixture of 3-nitroacetylacetone and acetylacetone to facilitate the spontaneous combustion reaction [34]. It is reported that the introduction of 3-nitroacetylacetone also improves the films quality. Mixtures of 2-methoxyethanol and acetylacetone with the addition of an aqueous ammonia solution have also been used to obtain IGZO films [ [35] (by spraying a mixture of precursors followed by decomposition), as well as compounds "related" to this system [36] or other oxide materials [37]. The use of organic additives as co-fuels (sorbitol, sucrose and $\beta$-glucose) to obtain IGZO thin films [38] or polymer additives [39] has been reported.

As for the case of obtaining IGZO in the form of single nanoparticles, such works are extremely rare [40, 41]. Previously, our team published a series of papers demonstrating that the phase composition and final morphology of the material can be influenced by the choice of complexing agent used in the synthesis. It was found that ethylene glycol, glycerol and tartaric acid are suitable for obtaining IGZO - their use leads to the formation of a powder without any crystallite impurities [42, 43]. The use of many other organic complexing agents (citric and oxalic acid, urea, sucrose, fructose [42], EDTA and ascorbic acid – *unpublished data* of our group) led to the appearance of foreign crystalline impurities (indium oxide) in the final powders.

The aim of this work is synthesis of $InGaZn_2O_5$ using method previously successfully tested (see [43]), and to study the properties of the obtained material.

## 2. Preparation and characterization method

The following reagents were used in the work: indium nitrate hydrate [$In(NO_3)_3 \cdot xH_2O$ (chemically pure)], gallium nitrate hydrate [$Ga(NO_3)_3 \cdot xH_2O$ (chemically pure)], zinc nitrate hydrate [$Zn(NO_3)_2 \cdot xH_2O$ (chemically pure)] and tartaric acid (analytical grade). All salts were preliminarily determined gravimetrically. The masses of the precursor samples were calculated from the ratio of metal cations $In^{3+}$:$Ga^{3+}$:$Zn^{2+}$ = 1:1:2 in the final ternary oxide. Samples were selected using a Joanlab FA2204N analytical balance. An IKA C-MAG HS7 magnetic stirrer with heating was used for stirring and evaporating the solutions of the mixture. The synthesis and thermal treatment of the xerogel obtained by evaporation of the initial mixture was carried out according to the method [44]. The samples were sintered in corundum crucibles at 700 °C and 900 °C for 12 hours. The samples were cooled in the furnace to 200 °C and then in air. The sintering temperatures are reflected in the names of the samples, which are discussed later.

X-ray diffraction (XRD) pattern of IGZO was collected on a Drawell DW-XRD-2700A powder diffractometer (Cu K$\alpha$, 40 kV, 30 mA, Ni filter) in the $2\theta$ angle range from 5° to 90° at a rate of 1 deg/min at room temperature. The size and

morphology of the particles were studied using Jeol JSM 7001F scanning electron microscopy (SEM) with accelerating voltage = 20 kV), the distribution of the main elements of the batch was studied using an Oxford X-Max 80 energy dispersive analyzer (EDS method) combined with a SEM. The crystalline structure of the particles was studied by Jeol JSM-2100 transmission electron microscopy (TEM) with accelerating voltage = 160 kV. IR- spectroscopy was performed using a Shimadzu IRAffinity-1S FTIR spectrometer (from 4000 to 400 $cm^{-1}$ in transmission mode). The background calibration was made for pure analytical grade KBr. The material was pressed into a tablet 13 mm in size and 1–1.5 mm thick. The content of indium gallium zinc oxide in the tablet was about 3...5 wt. %. A Shimadzu UV-2700 UV-Vis spectrophotometer was used to record diffuse reflectance spectra in the range from 250 to 800 nm at a recording rate of 1 nm/sec. The background calibration was performed for a pure barium sulfate $BaSO_4$ tablet. The sample was deposited on the barium sulfate tablet. The obtained diffuse reflectance spectra were used to calculate the band gap parameter (Kubelka-Munk transformation was applied under the assumption of a optically allowed direct bandgap).

## 3. Results and discussion

Fig. 1 shows the XRD patterns of the sample heat-treated at 500 °C, 700 °C and 900 °C. It can be seen from Fig. 1 that the general appearance of the diffraction pattern corresponds to the literature data for $InGaZn_2O_5$ [45, 46]. Over the entire range of sintering temperatures, the sample is single-phase and does not contain any extraneous reflections. Note that sintering at 900 °C is necessary to demonstrate the homogeneity of the material at lower temperatures, since the use of other complexing agents (e.g., urea) can lead to the formation of amorphous agglomerates of impurity phases that remain in the amorphous state up to temperatures of 900 °C [42]. At the same time, we do not exclude the possibility of a chemical reaction occurring at sintering temperatures of 700 and 900 °C if the sample is multiphase at a temperature of 500 °C. This will be discussed in the next section. It is easy to notice that the full width at half maximum of each individual reflex decreases with increasing processing temperature, which can be associated with an increase of crystallinity and grain growth. Thus, the sample obtained at 500 °C is X-ray amorphous, at 700 °C – weakly crystallized, at 900 °C – crystallized.

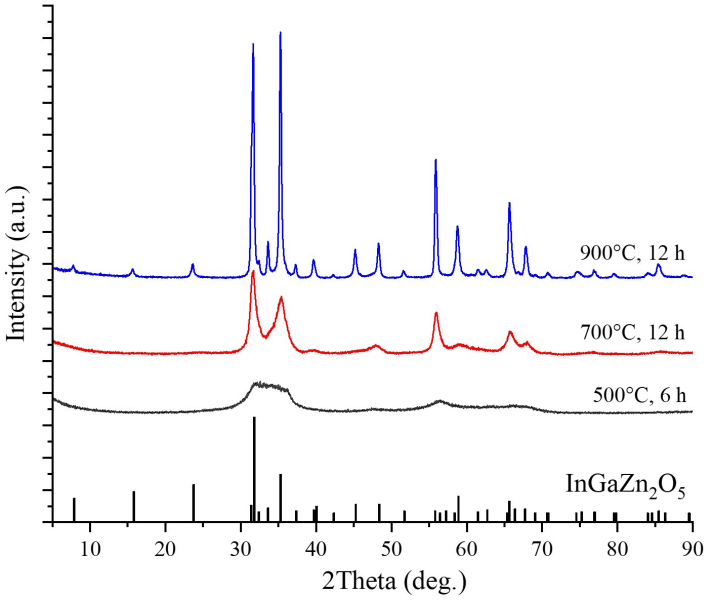


FIG. 1. XRD pattern of the $InGaZn_2O_5$ sample obtained at different temperatures, explanation in the legend

The morphology, size of agglomerates and particles of the $InGaZn_2O_5$ sample subjected to heat treatment at 500 °C for 6 hours were studied by SEM method in secondary electron contrast. In Fig. 1a, at x5000 magnification, particles from less than one to ten micrometres are visible. The shape of the particles is three dimensional, with distinct edges. The structure is non-uniform, with large structural elements and medium and small elements. At higher magnification, in Figs. 2(b-c), particles smaller than 100 nm are visible in the same area of the surface of large agglomerate. The structure of the agglomerate is very dense and uniform and the pores are not visible.

Fig. 3 shows the results of the EDS analysis. The chemical composition does not depend on the heat treatment temperature of the sample and shows a uniform distribution of the elements contained in the ternary oxide. The calculated formula of the compound indicates the proximity of the actual composition to the target, derived from the composition of the batch – $In_{1.01}Ga_{0.96}Zn_{2.03}O_5$. Thus, the chemical composition data are presented within the determined error limits and it can be stated that the sample corresponds to the specified composition.

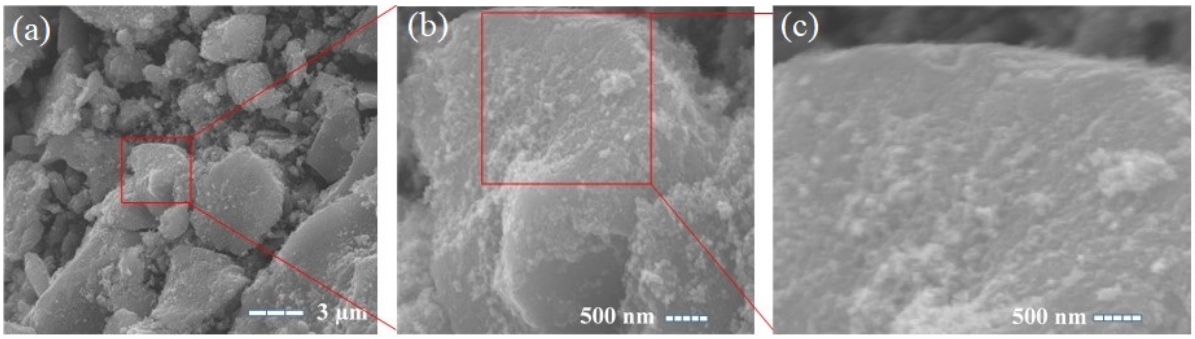


FIG. 2. SEM image of $InGaZn_2O_5$ sample sintered at 500 °C for 6 hours

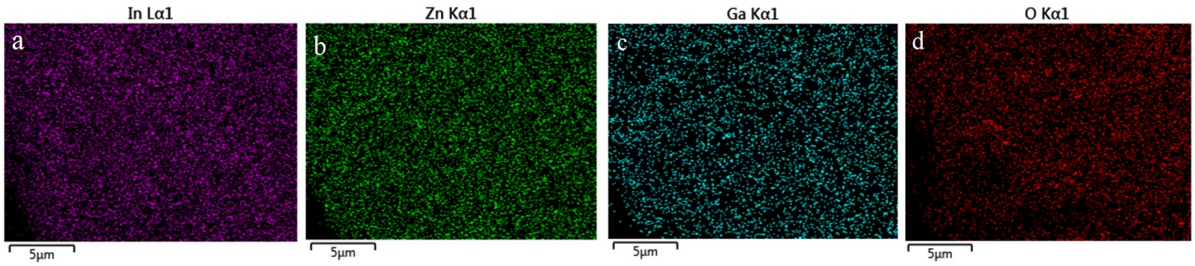


FIG. 3. EDS map of element distribution of In (a), Ga (b), Zn (c) and O (d)

Fig.4 and Fig. 5 show the results of transmission electron microscopy. As can be seen from Fig. 4, the sample is an agglomerate of small (approximately 4–8 nm) spherical-like nanoparticles. On a larger scale, in Fig. 5, it is clear that the particles are crystalline. Thus, it can be stated that a crystalline product is already formed at a temperature of 500 °C, with the degree of crystallinity increasing as the sintering temperature increases (according to X-ray diffraction data). At the same time, the coherent scattering region volume is low in the nanoparticles, so that the $InGaZn_2O_5$ sample sintered at 500 °C is X-ray amorphous.

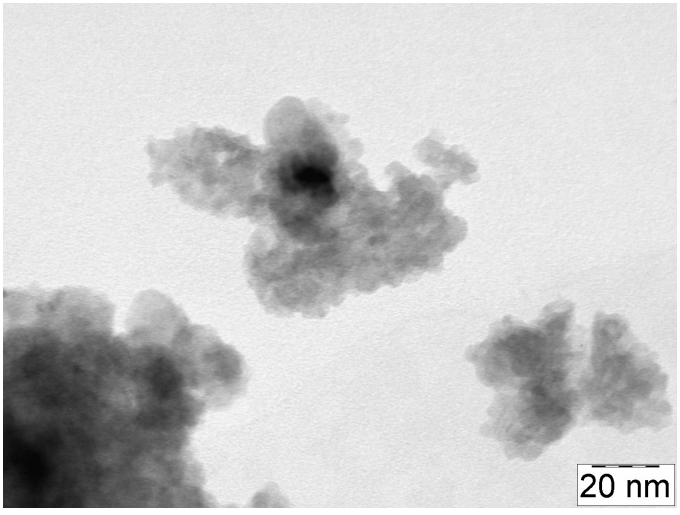


FIG. 4. TEM images of $InGaZn_2O_5$ sintered at 500 °C for 6 hours (low resolution)

The sample sintered at 500 °C was studied by IR-spectroscopy. The data is presented in the form of a detailed text description. A series of wavenumbers were recorded: from 3650 to 3000, 2900, 2700, 2400...2280, 1740...1280, 620, 430 $cm^{-1}$. A broad absorption peak in the region of 3650 to 3000 $cm^{-1}$ corresponds to the stretching vibrations of the "–OH" bond, which may indicate either the presence of the presence of adsorbed water bound water in the material or the presence of oxyhydroxides in the material. Two low intensity absorption bands were found in the region of 2900 and 2700 $cm^{-1}$, apparently the region of the stretching vibrations of the "–CH" bond, most likely due to contamination of the samples with ethanol used for sample preparation. Absorption bands of carbon dioxide CO2 were recorded in the region from 2400 to 2280 $cm^{-1}$. The sample also had an absorption peak in the region of lower wave numbers from

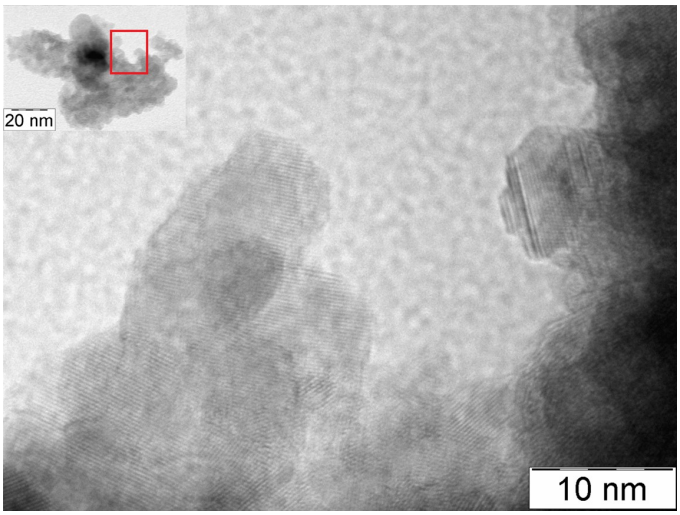


FIG. 5. TEM image of $InGaZn_2O_5$ sintered at 500 °C for 6 hours (high resolution)

1740 to 1280 $cm^{-1}$, which most likely corresponds to the "–C=O" bond, indicating the presence of tartaric acid oxidation products in the samples, which cannot be removed at a temperature of 500 °C and exposure of 6 hours. Alternatively, this peak may correspond to the "C–C" bond, which may indicate the same thing. The most informative part of the spectrum is the region from 600 to 300 $cm^{-1}$, as it contains information about the Me–O bonds. In our analysis, the 600 to 400 $cm^{-1}$ region was examined only, due to hardware limitations. In this region, an absorption peak at ≈630 $cm^{-1}$ is observed which can be attributed to the In–O or Ga–O bond. The peak at ≈420 $cm^{-1}$ could not be clearly interpreted.

A diffuse reflectance UV-Vis spectrum was recorded for the sample sintered at 500 °C. As can be seen from the data (Fig. 6), no significant light absorption was detected in the near IR and visible range from 800 to 300 nm. This correlates with the appearance of the sample, which is presented as white powder with yellowish tinge. The data for the UV-Vis diffuse reflectance spectra obtained were used to calculate the optical band gap, which was found to be 3.10 eV, in little disagreement with data from previously published work on the same IGZO composition [47], with the difference about 0.15 eV.

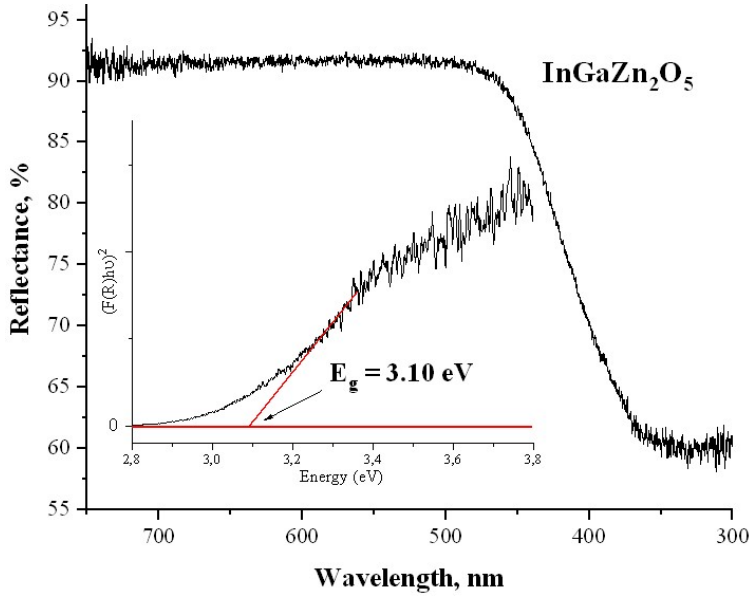


FIG. 6. UV-Vis spectrum and Tauc plot (insert) for determining the optical band gap of $InGaZn_2O_5$

## 4. Conclusion

The nitrate-tartrate complex decomposition method has been successfully applied to the process of obtaining $InGaZn_2O_5$. The use of tartaric acid as a chelating reagent in nitrate-organic complex decomposition method leads to the formation of a nanocrystalline material at a sintering temperature of 500 °C. Using electron microscopy (SEM and

TEM), it was found that the material sintered at 500 °C is an agglomerate of nanoparticles, the morphology of individual nanoparticles being close to spherical. As the sintering temperature increases, the degree of crystallinity of the material increases, at 900 °C the material is well crystallized according to the XRD data. The distribution of the main elements in the material is homogeneous according to EDS data. The IR-spectrum confirms the presence of Me–O bonds in the material. The band gap for the $InGaZn_2O_5$ sample sintered at 500 °C is 3.10 eV.

## References


[1] Zhang Z., Zou R., Yu L., Hu J. Recent research on one-dimensional silicon-based semiconductor nanomaterials: Synthesis, structures, properties and applications. *Crit. Rev. Solid State Mater. Sci.*, 2011, **36**(3), P. 148–173.

[2] Balaghi L., Shan S., Fotev I., Moebus F., Rana R., Venanzi T., Hübner R., Mikolajick T., Schneider H., Helm M., Pashkin A., Dimakis E. High electron mobility in strained GaAs nanowires. *Nat. Commun.*, 2021, **12**, P. 6642.

[3] Khan M.A.H., Rao M.V. Gallium Nitride (GaN) Nanostructures and their gas sensing properties: A review. *Sensors.*, 2020, 20(14), P. 3889.

[4] Potts H., Morgan N.P., Tutuncuoglu G., Friedl M., Morral A.F.i. Tuning growth direction of catalyst-free InAs(Sb) nanowires with indium droplets. *Nanotechnology*., 2017, 28(5), P. 054001.

[5] Li X., Zhu H. Two-dimensional MoS2: Properties, preparation, and applications. *J. Materiomics.*, 2015, 1(1), P. 33–44.

[6] Patoary N.H., Xie J., Zhou G., Mamun F.Al., Sayyad M., Tongay S., Esqueda I.S. Improvements in 2D p-type WSe2 transistors towards ultimate CMOS scaling. *Sci. Rep.*, 2023, **13**, P. 3304.

[7] Yu Z., Perera I.R., Daeneke T., Makuta S., Tachibana Y., Jasieniak J.J., Mishra A., Bäuerle P., Spiccia L., Bach U. Indium tin oxide as a semiconductor material in efficient p-type dye-sensitized solar cells. *NPG Asia Mater.*, 2016, **8**(8), P. e305–e305.

[8] Cheng C.-H., Tsay C.-Y., Flexible a-IZO thin film transistors fabricated by solution processes. *J. Alloys Compd.*, 2010, **507**(1), P. L1–L3.

[9] Bastola A., He Y., Im J., Rivers G., Wang F., Worsley R., Austin J.S., Nelson-Dummett O., Wildman R.D., Hague R., Tuck C.J., Turyanska L. Formulation of functional materials for inkjet printing: A pathway towards fully 3D printed electronics. *Mater. Today Electron.*, 2023, **6**, P. 100058.

[10] Kaçar R., Serin R.B., Uçar E., Ülkü A. A review of high-end display technologies focusing on inkjet printed manufacturing. Mater. *Today Commun.*, 2023, **35**, P. 105534.

[11] Bhatti G., Agrawal Y., Palaparthy V., Kavicharan M., Agrawal M. Chapter 13 - Flexible Electronics: A Critical Review. In: Agrawal Y., Mummaneni K., Sathyakam P.U., editors. Interconnect Technologies for Integrated Circuits and Flexible Electronics. Springer Tracts in Electrical and Electronics Engineering. Springer, Singapore. 2024, P. 221–248.

[12] Bi S., Gao B., Han X., He Z.R., Metts J., Jiang C.M., Asare-Yeboah K. Recent progress in printing flexible electronics: A review. *Sci. China Technol. Sci.*, 2024, **67**(8), P. 2363–2386.

[13] Samanta S., Han K., Sun C., Wang C., Thean A.V.-Y., Gong X. Amorphous IGZO TFTs Featuring Extremely-Scaled Channel Thickness and 38 nm Channel Length: Achieving Record High Gm,max of 125 $\mu$S/$\mu$m at VDS of 1 V and ION of 350 $\mu$A/$\mu$m. In Proc. IEEE Symp. VLSI Technol., 2020, P. 1–2.

[14] Yin X., Ji X., Liu W., Li X., Wang M., Xin Q., Zhang J., Yan Z., Song A. Electrolyte-gated amorphous IGZO transistors with extended gates for prostate-specific antigen detection. *Lab. Chip.*, 2024, **24**, P. 3284–3293.

[15] Sheng J., Hong T., Lee H.-M., Kim K., Sasase M., Kim J., Hosono H., Park J.-S. Amorphous IGZO TFT with High Mobility of $\sim$70 cm2/(V s) via Vertical Dimension Control Using PEALD. ACS Appl. Mater. Interfaces., 2019, **11**(43), P. 40300–40309.

[16] Han Y., Lee D.H., Cho E.-S., Kwon S.J., Yoo H. Argon and Oxygen Gas Flow Rate Dependency of Sputtering-Based Indium-Gallium-Zinc Oxide Thin-Film Transistors. Micromachines, 2023, **14**(7), P. 1394.

[17] Nomura K., Ohta H., Takagi A., Kamiya T., Hirano M., Hosono H. Room-temperature fabrication of transparent flexible thin-film transistors using amorphous oxide semiconductors. *Nature*, 2004, **432**(7016), P. 488–492.

[18] Wager J.F., Yeh B., Hoffman R.L., Keszler D.A. An amorphous oxide semiconductor thin-film transistor route to oxide electronics. *Curr. Opin. Solid State Mater. Sci.*, 2014, **18**(2), P. 53–61.

[19] Chiang H.Q., Wager J.F., Hoffman R.L., Jeong J., Keszler D.A. High mobility transparent thin-film transistors with amorphous zinc tin oxide channel layer. *Appl. Phys. Lett.*, 2004, **86**(1), P. 13503.

[20] Venkateshvaran D., Nikolka M., Sadhanala A., Lemaur V., Zelazny M., Kepa M., Hurhangee M., Kronemeijer A.J., Pecunia V., Nasrallah I., Romanov I., Broch K., McCulloch I., Emin D., Olivier Y., Cornil J., Beljonne D., Sirringhaus H. Approaching disorder-free transport in high-mobility conjugated polymers. *Nature*, 2014, **515**(7527), P. 384–388.

[21] Fukuda K., Takeda Y., Yoshimura Y., Shiwaku R., Tran L.T., Sekine T., Mizukami M., Kumaki D., Tokito S. Fully-printed high-performance organic thin-film transistors and circuitry on one-micron-thick polymer films. *Nat. Commun.*, 2014, **5**(1), P. 4147.

[22] Giri G., DeLongchamp D.M., Reinspach J., Fischer D.A., Richter L.J., Xu J., Benight S., Ayzner A., He M., Fang L., Xue G., Toney M.F., Bao Z. Effect of solution shearing method on packing and disorder of organic semiconductor polymers. *Chem. Mater.*, 2015, **27**(7), P. 2350–2359.

[23] Yan H., Chen Z., Zheng Y., Newman C., Quinn J.R., Dötz F., Kastler M., Facchetti A. A high-mobility electron-transporting polymer for printed transistors. *Nature*, 2009, **457**(7230), P. 679–686.

[24] Takeda Y., Yoshimura Y., Shiwaku R., Hayasaka K., Sekine T., Okamoto T., Matsui H., Kumaki D., Katayama Y., Tokito S. Organic complementary inverter circuits fabricated with reverse offset printing. *Adv. Electron. Mater.*, 2018, **4**(1), P. 1700313.

[25] Shiwaku R., Takeda Y., Fukuda T., Fukuda K., Matsui H., Kumaki D., Tokito S. Printed 2 V-operating organic inverter arrays employing a small-molecule/polymer blend, Sci. Rep., 2016, **6**(1), P. 34723.

[26] Minemawari H., Yamada T., Matsui H., Tsutsumi J., Haas S., Chiba R., Kumai R., Hasegawa T. Inkjet printing of single-crystal films. *Nature*, 2011, **475**(7356), P. 364–367.

[27] Zhang W., Smith J., Watkins S.E., Gysel R., McGehee M., Salleo A., Kirkpatrick J., Ashraf S., Anthopoulos T., Heeney M., McCulloch I. Indacenodithiophene semiconducting polymers for high-performance, air-stable transistors. *J. Am. Chem. Soc.*, 2010, **132**(33), P. 11437–11439.

[28] Zeng H., Rice P.M., Wang S.X., Sun S. Shape-controlled synthesis and shape-induced texture of MnFe2O4 nanoparticles. *J. Am. Chem. Soc.*, 2004, **126**(37), P. 11458–11459.

[29] Sun S., Zeng H., Robinson D.B Raoux S., Rice P.M., Wang S.X., Li G. Monodisperse $MFe_2O_4$ (M=Fe, Co, Mn) Nanoparticles. *J. Am. Chem. Soc.*, 2004, **126**(1), P. 273–279.

[30] Vinnik, D.A., Kovalev, A.I., Sherstyuk, D., Zhivulin, D.E., Zirnik, G.M., Batmanova T. Development of a scalable method for synthesizing a promising oxide material for electronics In-Ga-Zn-O, RusMetal, 2024.

[31] Yoon S., Kim S.J., Tak Y.J., Kim H.J. A solution-processed quaternary oxide system obtained at low-temperature using a vertical diffusion technique. *Sci. Rep.*, 2017, **7**(1), P. 43216.

[32] Sanctis S., Hoffmann R.C., Koslowski N., Foro S., Bruns M., Schneider J.J. Aqueous Solution Processing of Combustible Precursor Compounds into Amorphous Indium Gallium Zinc Oxide (IGZO) Semiconductors for Thin Film Transistor Applications. *Chem. Asian J.*, 2018, **13**(24), P. 3912–3919.
[33] Xie Y., Wang D., Fong H.H. High-Performance Solution-Processed Amorphous InGaZnO Thin Film Transistors with a Metal–Organic Decomposition Method. *J. Nanomater.*, 2018, **2018**, P. 7423469.
[34] Chen Y., Wang B., Huang W., Zhang X., Wang G., Leonardi M.J., Huang Y., Lu Z., Marks T.J., Facchetti A. Nitroacetylacetone as a Cofuel for the Combustion Synthesis of High-Performance Indium–Gallium–Zinc Oxide Transistors. *Chem. Mater.*, 2018, **30**(10), P. 3323–3329.
[35] Wang B., Yu X., Guo P., Huang W., Zeng L., Zhou N., Chi L., Bedzyk M.J., Chang R.P.H., Marks T.J., Facchetti A. Solution-Processed All-Oxide Transparent High-Performance Transistors Fabricated by Spray-Combustion Synthesis. *Adv. Electron. Mater.*, 2016, **2**(4), P. 1500427.
[36] Kim M.-G., Kanatzidis M.G., Facchetti A., Marks T.J. Low-temperature fabrication of high-performance metal oxide thin-film electronics via combustion processing. Nat. Mater., 2011, **10**(5), P. 382–388.
[37] Hennek J.W., Kim M.-G.,, Kanatzidis M.G., Facchetti A., Marks T.J. Exploratory Combustion Synthesis: Amorphous Indium Yttrium Oxide for Thin-Film Transistors. *J. Am. Chem. Soc.*, 2012, **134**(23), P. 9593–9596.
[38] Wang B., Zeng L., Huang W., Melkonyan F.S., Sheets W.C., Chi L., Bedzyk M.J., Marks T.J., Facchetti A. Carbohydrate-Assisted Combustion Synthesis To Realize High-Performance Oxide Transistors. *J. Am. Chem. Soc.*, 2016, **138**(22), P. 7067–7074.
[39] Wang B., Huang W., Bedzyk M.J., Dravid V.P., Hu Y.Y., Marks T.J., Facchetti A. Combustion Synthesis and Polymer Doping of Metal Oxides for High-Performance Electronic Circuitry. *Acc. Chem. Res.*, 2022, **55**(3), P. 429–441.
[40] Fukuda N., Watanabe Y., Uemura S., Yoshida Y., Nakamura T., Ushijima H. In–Ga–Zn oxide nanoparticles acting as an oxide semiconductor material synthesized via a coprecipitation-based method. *J. Mater. Chem. C.*, 2014, **2**(13), P. 2448–2454.
[41] Wu M.-C., Hsiao K.-C., Lu H.-C. Synthesis of InGaZnO4 nanoparticles using low temperature multistep co-precipitation method. *Mater. Chem. Phys.*, 2015, **162**, P. 386–391.
[42] Zirnik G.M., Chernukha A.S., Uchaev D.A., Solizoda I.A., Gudkova S.A., Nekorysnova N.S., Vinnik D.A. Phase formation of nanosized InGaZnO4 obtained by the sol-gel method with different chelating agents. *Nanosyst. Physics, Chem. Math.*, 2024, **15**(4), P. 520–529.
[43] Zirnik G.M., Sozykin S.A., Uchaev D.A., Chernukha A.S., Solizoda I.A., Gudkova S.A., Vinnik D.A. Preparation and synthesis of polycrystalline InGaZnO4 via tartaric acid mediated sol-gel method. Russ. Metall, 2024.
[44] Zirnik G.M., Sozykin S.A., Chernukha A.S., Solizoda I.A., Gudkova S.A., Vinnik D.A. Indium gallium zinc oxide: Effect of complexing agent on structure. *Journal of Structural Chemistry*, 65(2024), P. 133998.
[45] Tien T.-C., Wu J.-S., Hsieh T.-E., Wu H.-J. The Fabrication of Indium–Gallium–Zinc Oxide Sputtering Targets with Various Gallium Contents and Their Applications to Top-Gate Thin-Film Transistors. *Coatings.*, 2022, **12**(8), P. 1217.
[46] Kimizuka N., Mohri T., Matsui Y., Siratori K. Homologous compounds, InFeO3(ZnO)m (m=1–9). *J. Solid State Chem.*, 1988, **74**(1), P. 98–109.
[47] Préaud S., Byl C., Brisset F., Berardan D. SPS-assisted synthesis of InGaO3(ZnO) ceramics, and influence of m on the band gap and the thermal conductivity. *J. Am. Ceram. Soc.*, 2020, **103**(5), P. 3030–3038.

*Submitted 14 October 2024; accepted 11 February 2025*

*Information about the authors:*

*Gelena M. Boleiko* – Moscow Institute of Physics and Technology Institutsky lane, 9, Dolgoprudny, 141701, Russia; ORCID 0009-0003-3438-5893; boleiko.gm@mipt.ru

*Gleb M. Zirnik* – Moscow Institute of Physics and Technology Institutsky lane, 9, Dolgoprudny, 141701, Russia; ORCID 0009-0008-4546-1368; glebanaz@mail.ru

*Andrey I. Kovalev* – Moscow Institute of Physics and Technology Institutsky lane, 9, Dolgoprudny, 141701, Russia; South Ural State University, Lenin Av., 76, Chelyabinsk, 454080, Russia; ORCID 0009-0003-4773-1687; asp23kai165@susu.ru

*Daniil A. Uchaev* – South Ural State University, Lenin Av., 76, Chelyabinsk, 454080, Russia; ORCID 0000-0002-8623-4769; uchaevda@susu.ac.ru

*Ibrohimi A. Solizoda* – Moscow Institute of Physics and Technology Institutsky lane, 9, Dolgoprudny, 141701, Russia; St. Petersburg State University Universitetskaya embankment, 7-9, 199034, St. Petersburg; Tajik National University Rudaki Av., 17, Dushanbe, 734025, Tajikistan; ORCID 0000-0001-6973-4633; solizoda.ia@mipt.ru

*Alexander S. Chernukha* – Moscow Institute of Physics and Technology Institutsky lane, 9, Dolgoprudny, 141701, Russia; South Ural State University, Lenin Av., 76, Chelyabinsk, 454080, Russia; ORCID 0000-0002-1272-1628; chernukha.as@mipt.ru

*Svetlana A. Gudkova* – Moscow Institute of Physics and Technology Institutsky lane, 9, Dolgoprudny, 141701, Russia; St. Petersburg State University Universitetskaya embankment, 7-9, 199034, St. Petersburg; ORCID 0000-0002-3028-947X; svetlanagudkova@yandex.ru

*Denis A. Vinnik* – Moscow Institute of Physics and Technology Institutsky lane, 9, Dolgoprudny, 141701, Russia; South Ural State University, Lenin Av., 76, Chelyabinsk, 454080, Russia; St. Petersburg State University Universitetskaya embankment, 7-9, 199034, St. Petersburg; ORCID 0000-0002-5190-9834; vinnik.da@mipt.ru

*Conflict of interest*: the authors declare no conflict of interest.